

SUPPLEMENTARY INFORMATION

The Contributions of Molecular Vibrations and Higher Triplet Levels to the Intersystem Crossing Mechanism in Metal-Free Organic Emitters.

Rongjuan Huang,¹ João Avó,² Thomas Northey,⁴ E. Channing-Pearce,¹ Paloma L. dos-Santos,¹ Jonathan S. Ward,³ Przemyslaw Data,^{1,5} Marc K. Etherington,¹ Mark A. Fox,³ Thomas J. Penfold,⁴ Mário N. Berberan-Santos,⁶ João C. Lima,² Martin R. Bryce,³ and Fernando B. Dias^{1*}

¹Physics Department, Durham University, South Road, Durham, UK, DH1 3LE.

²REQUIMTE, Departamento de Química, Faculdade de Ciências e Tecnologia, Universidade Nova de Lisboa, 2829-516 Caparica, Portugal.

³Chemistry Department, Durham University, South Road, Durham, UK, DH1 3LE.

⁴School of Chemistry, Newcastle University, Newcastle upon Tyne, UK, NE1 7RU.

⁵Silesian University of Technology, Faculty of Chemistry, 44-100 Gliwice, Strzody 9, Poland

⁶Centro de Química-Física Molecular, Instituto Superior Técnico, 1049-001 Lisboa, Portugal

Email of corresponding author: f.m.b.dias@durham.ac.uk

Figure S1-(a) Steady-state emission spectra in solid ethanol solution at 100 K for compounds **1–10**. The compounds **1**, **3** and **5** show no phosphorescence, whereas their corresponding regioisomers show strong dual fluorescence-phosphorescence.

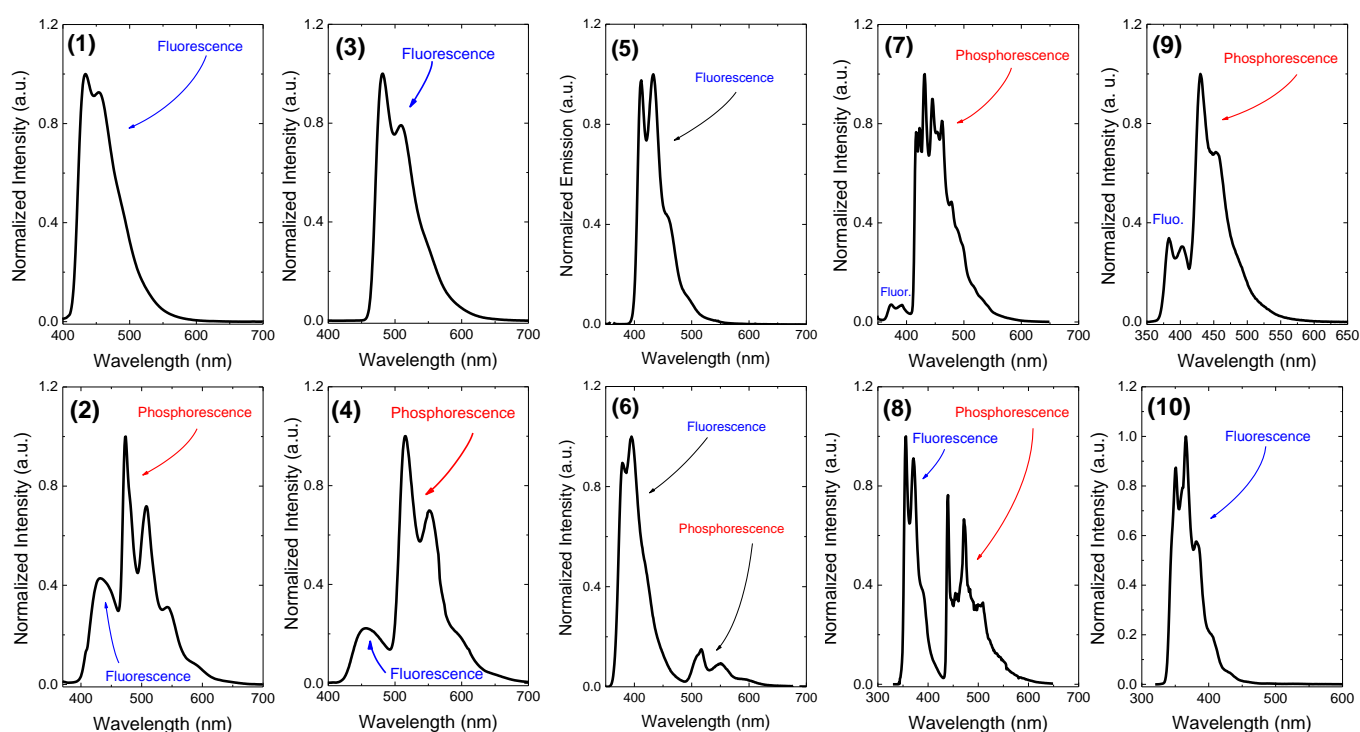
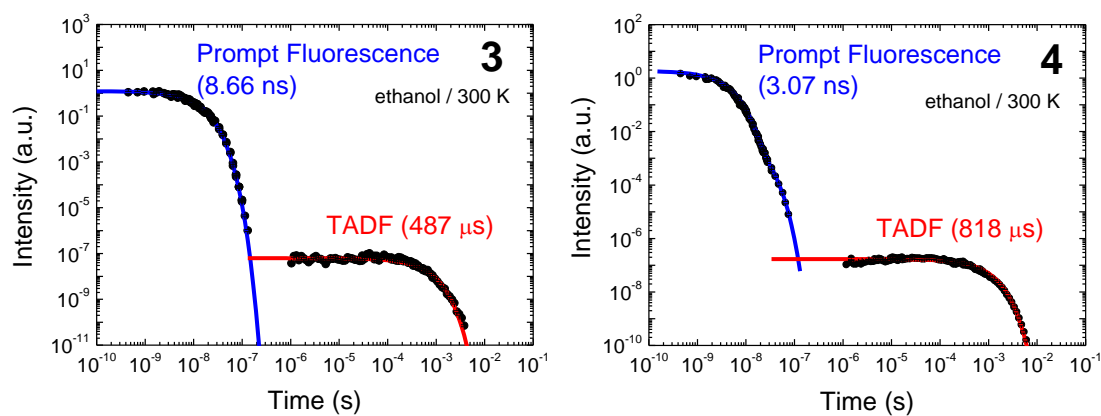


Figure S2- (a) Fluorescence decay showing prompt and delayed fluorescence components for compounds **3** and **4** in ethanol solution at 300 K. (b) Power dependence of the integrated delayed fluorescence in **3** and **4**. The slope in **3** is 2 whereas in **4** is 1, showing the different nature of the mechanisms that give origin to the delayed fluorescence, triplet-triplet annihilation (TTA) and TADF, respectively.

(a)



(b)

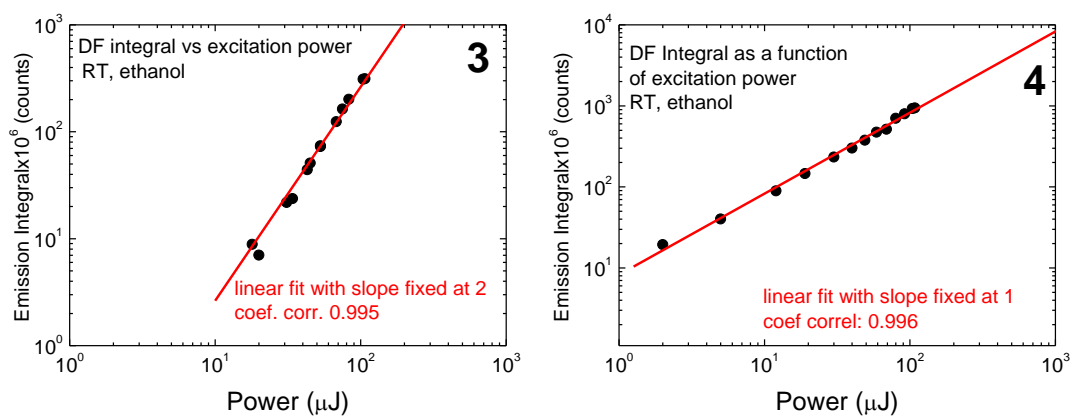


Figure S3- Steady-state emission in zeonex at 300 K in the presence of oxygen and in vacuum. Compounds **1**, **3**, and **5** show no phosphorescence at 300 K. However, their corresponding isomers show intense RTP. Compounds **7** and **8** are “angular” substituted and also show RTP. In **9**, instead of RTP, the increase of the fluorescence intensity upon degassing indicates the presence of TADF. Note that in all the compounds, with the exception of **9**, the intensity of the fluorescence band is practically not affected by presence/absence of oxygen.

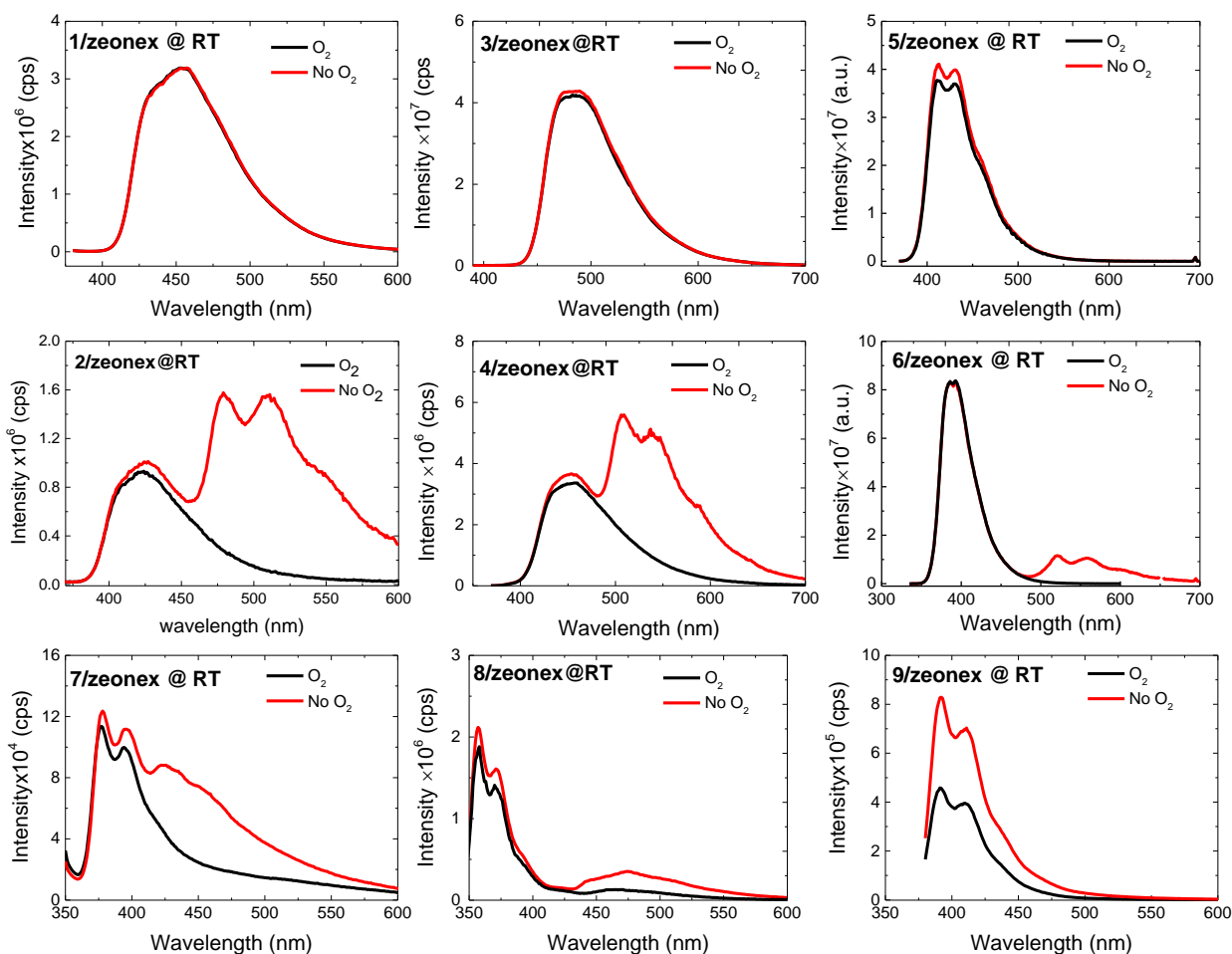


Figure S4- Fluorescence decays of compounds **1–4** in zeonex solid film at room temperature, collected at the fluorescence band.

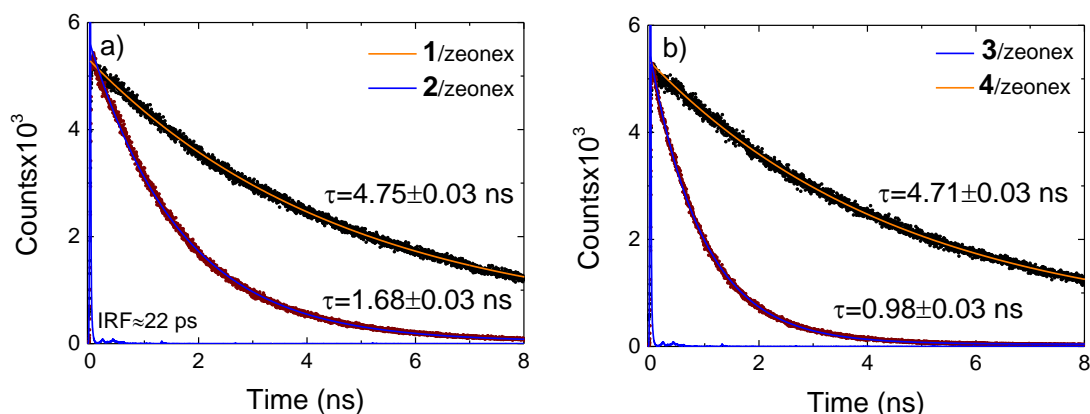


Figure S5- Fluorescence decays of compounds **2** and **4** in zeonex solid film at room temperature, collected at the phosphorescence band.

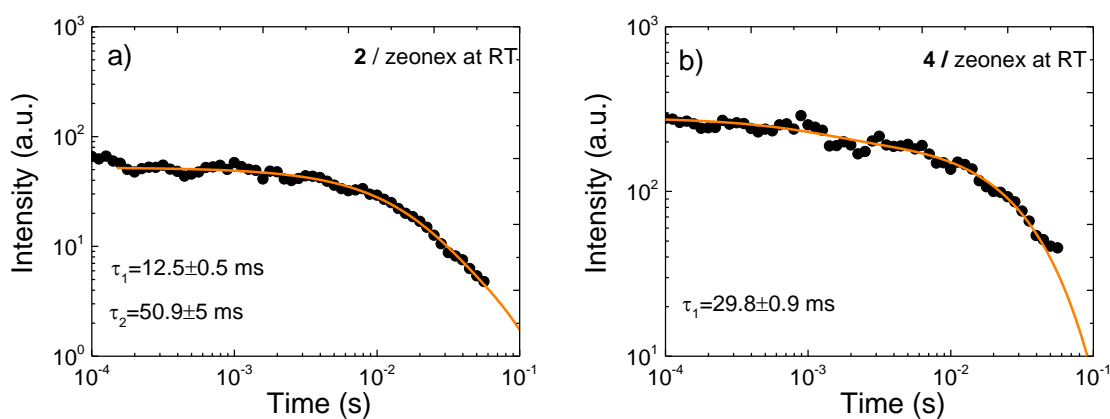
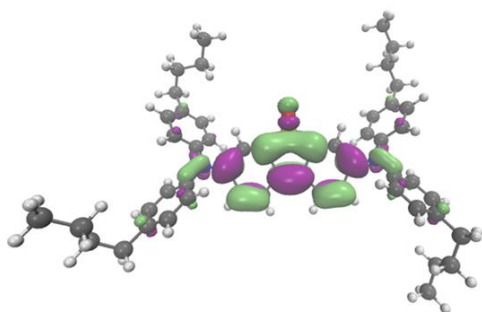
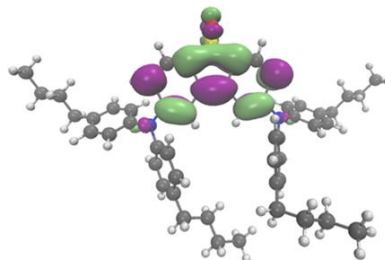


Figure S6-HOMO and LUMO contour plots for compounds **3–4**.

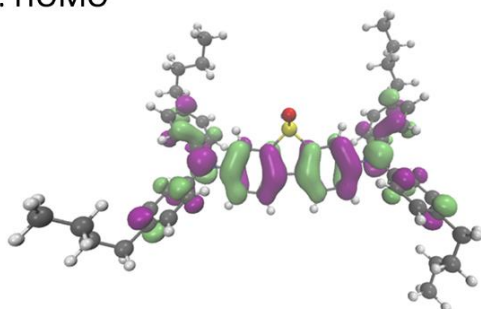
3: LUMO



4: LUMO



3: HOMO



4: HOMO

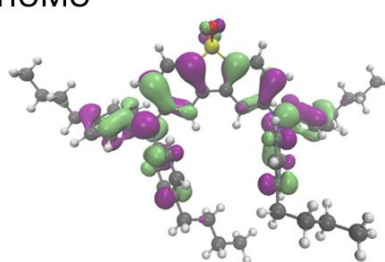


Figure S7- Molecular structures of hosts (a) TSP01 and (b) poly(4-bromostyrene) (PBrS).

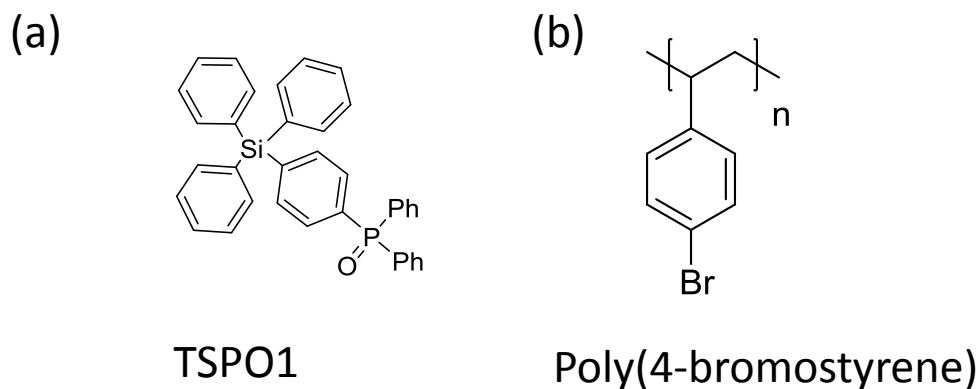


Figure S8- Steady-state emission spectra of compounds **1–4** dispersed in PBrS, in vacuum (red) and in air equilibrated (black) conditions at 300 K. Compounds **2** and **4** show dual luminescence, TADF and RTP, compounds **1** and **3** show only prompt fluorescence.

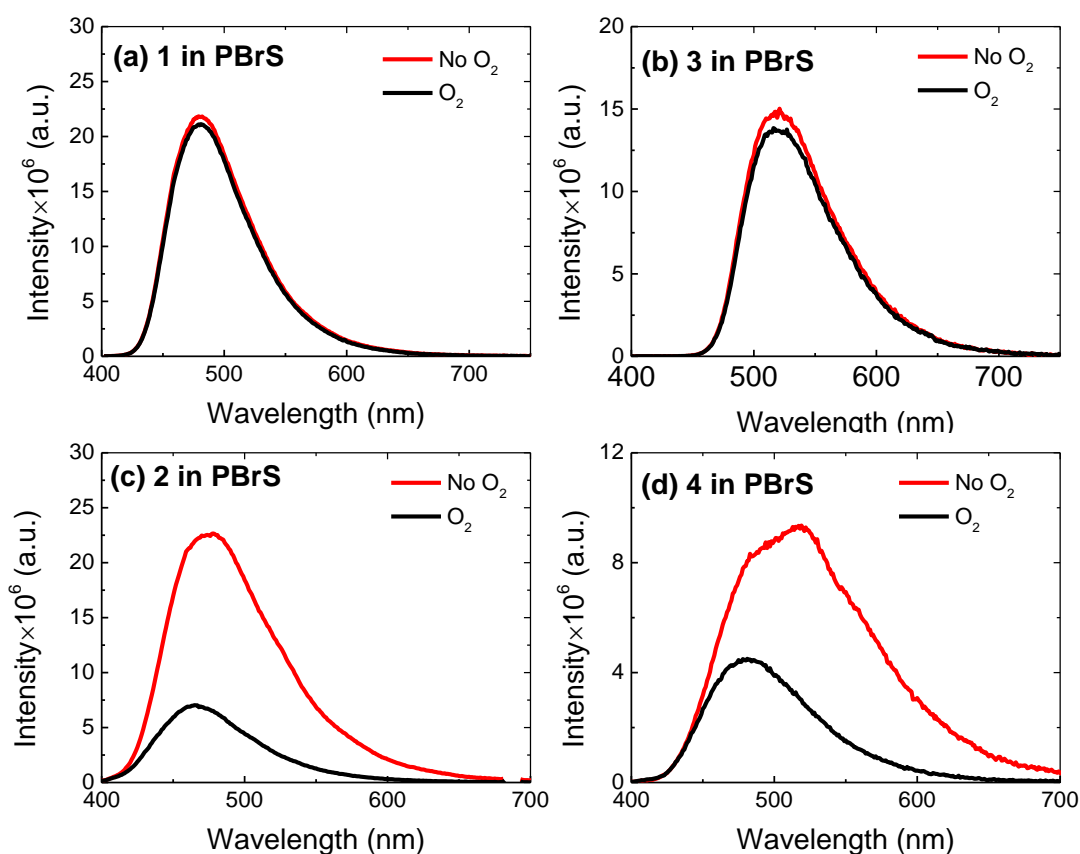


Figure S9- Steady-state emission spectra of compound **2** dispersed in different hosts (a) **7**, (b) **9**, (c) TSP01 and (d) PBrS, in vacuum (red) and air equilibrated (black) conditions.

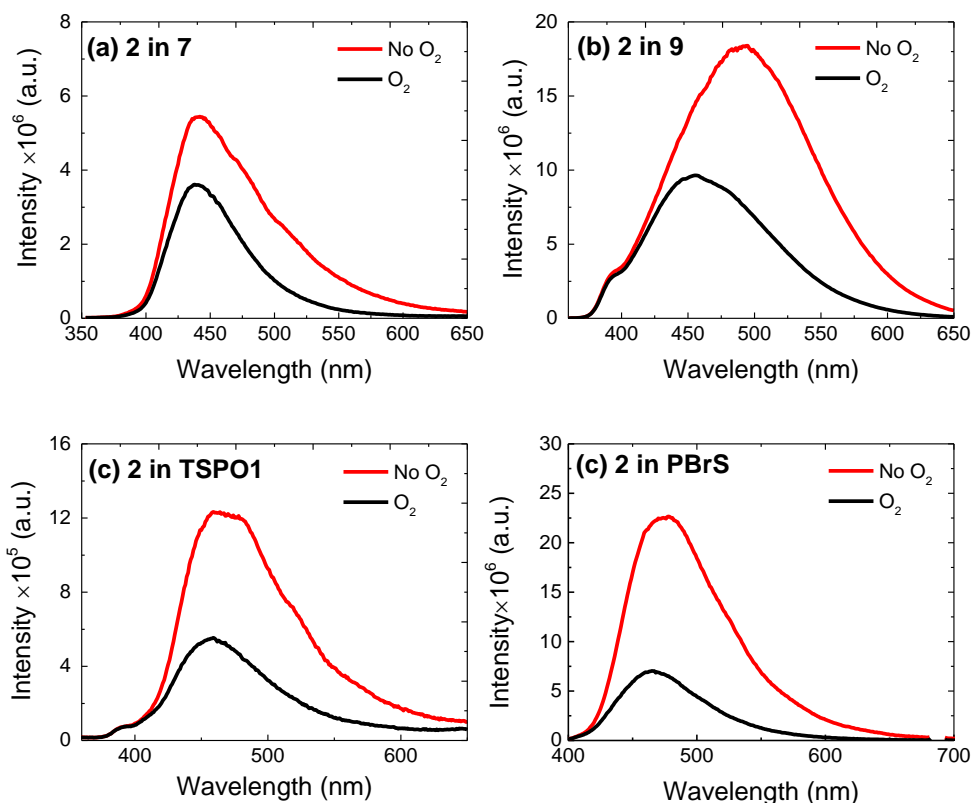


Figure S10- Time-resolved luminescence decays for compounds **2** and **4** dispersed in **7**, **9** and TSP01 hosts. In all cases long-lived dual luminescence is observed.

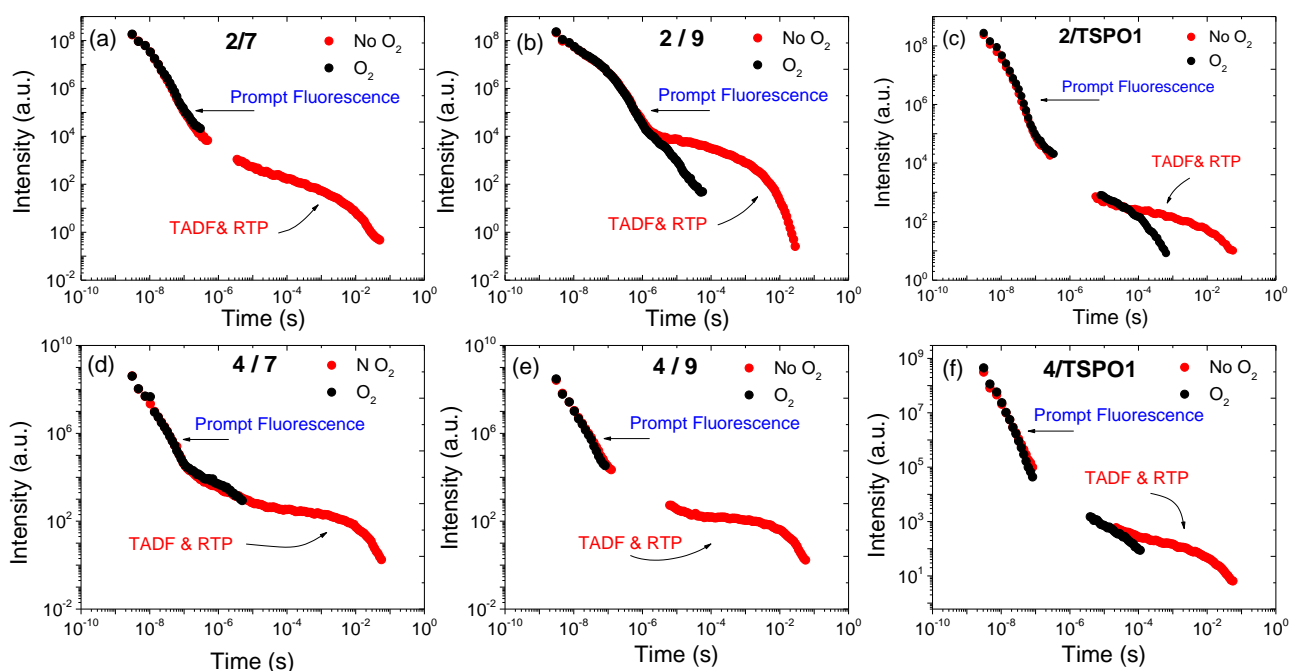


Figure S11- Time-resolved spectra of compounds **2** and **4** dispersed in **7**, **9** and TSPO1 showing the spectra of the prompt fluorescence (black), and long-lived TADF and RTP (red). Both spectra are compared with the steady-state emission spectra in zeonex (blue).

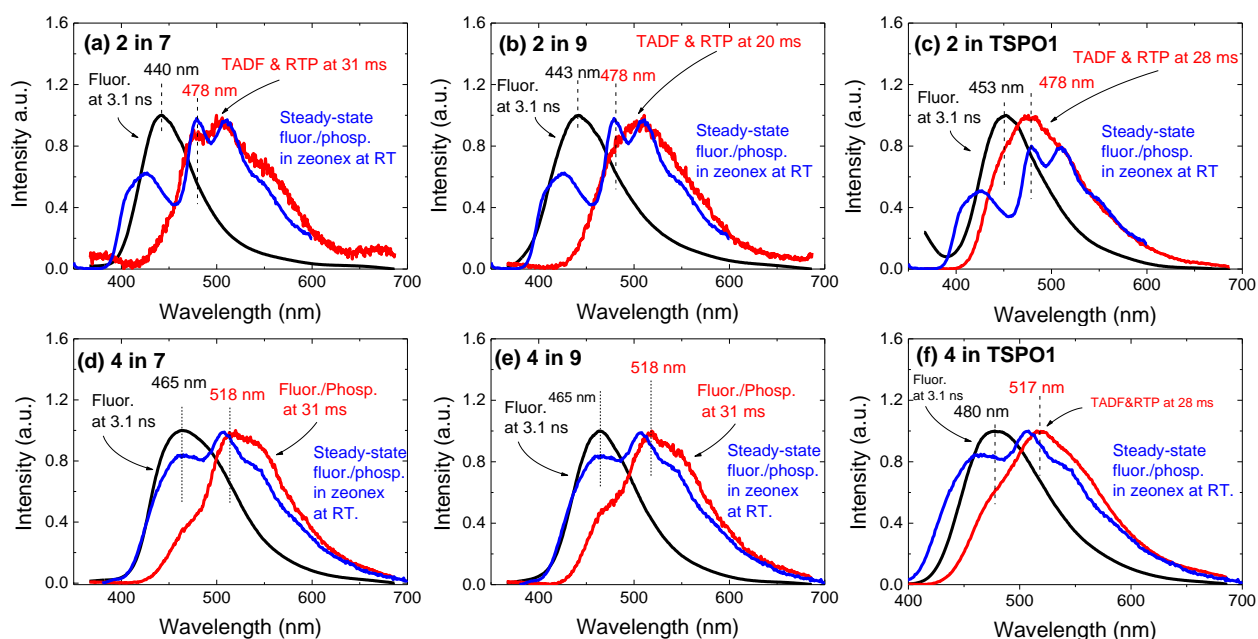


Figure S12- Triplet transient absorption decays for compounds **2**, **4** and **6-9** in deaerated *n*-hexane upon excitation at 355 nm followed at absorption maxima with (red) and without (black) β -carotene

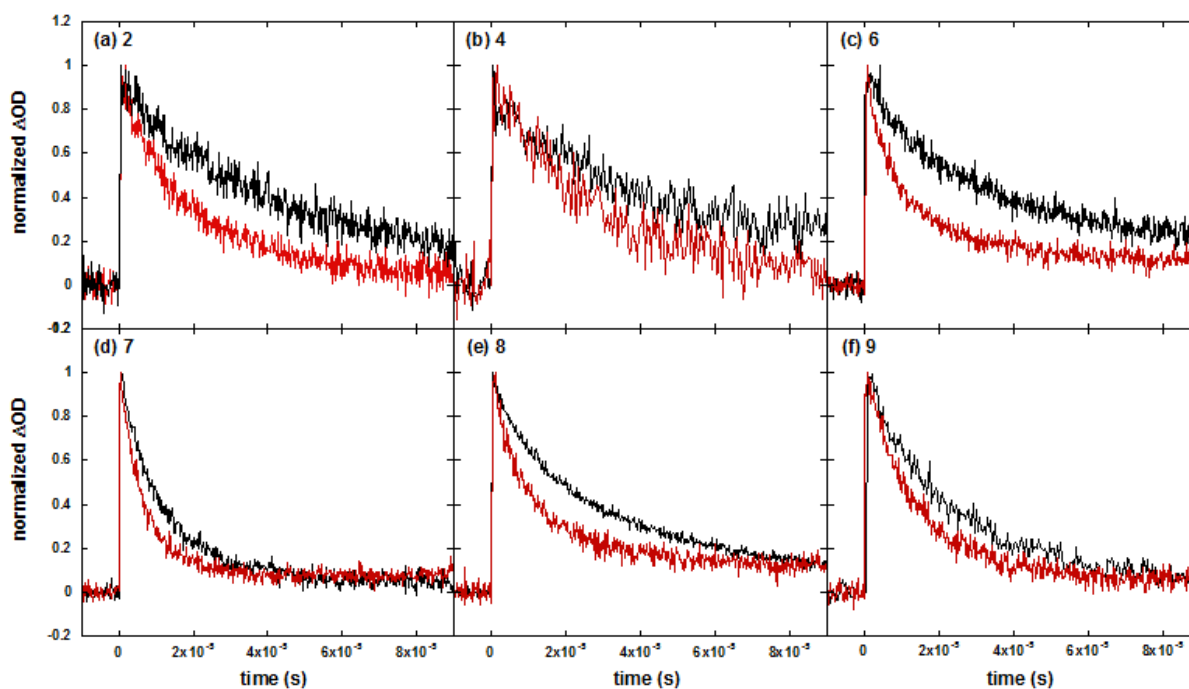


Figure S13- Triplet transient absorption spectra for compounds (a) **2**, (b) **4**, (c) **6**, (d) **7**, (e) **8** and (f) **9** in deaerated *n*-hexane with (red) and without (black) β -carotene as triplet quencher

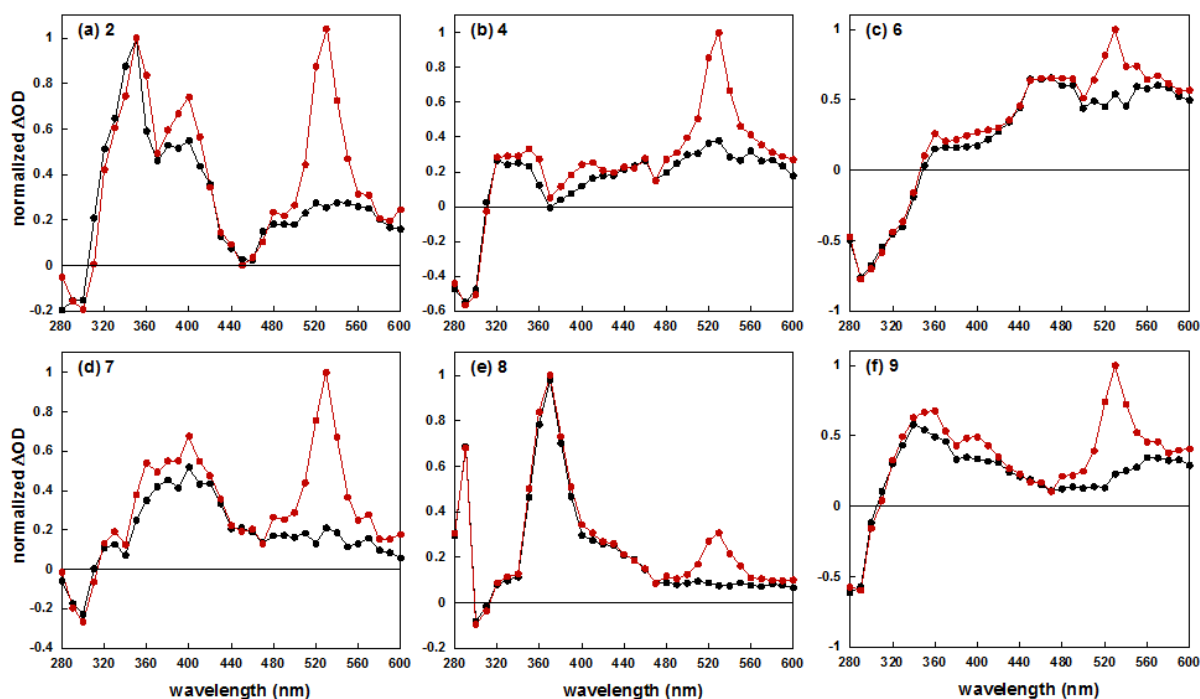
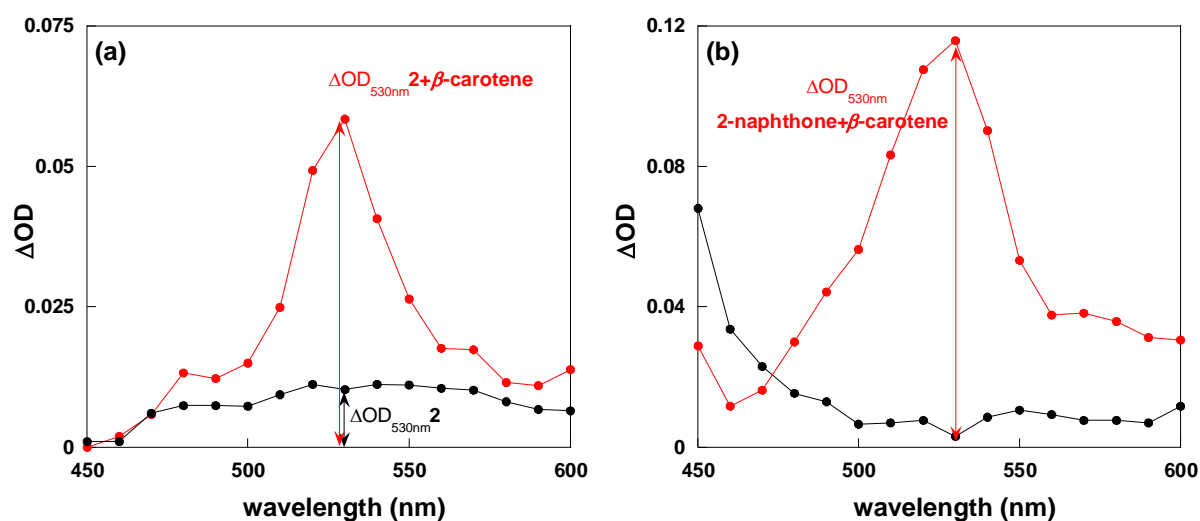


Figure S14 – Triplet transient absorption spectra for compound (a) **2** and (b) **2-naphthone** evidencing the increase in ΔOD at 530 nm in the presence of β -carotene.



From the decays in Figure S12, the efficiency of energy transfer from the standard P_{ET} (N) and the studied compounds, P_{ET} , to β -carotene can be determined by measuring the triplet lifetime of the donor in the absence (τ_{T0}) and in the presence (τ_T) of β -carotene, as in equation S1

$$P_{ET} = \frac{\tau_T^0 - \tau_T'}{\tau_T^0} \quad \text{S1}$$

The change in absorbance at 530 nm in the transient spectra of Figure S13 allows the determination of the relative concentration of β -carotene triplet formed upon excitation of the studied compounds compared to the standard in the same conditions, as in equation S2.

$$[\beta\text{-carotene}] = \frac{\Delta OD_{(\beta\text{-carotene})} - \Delta OD}{\Delta OD_{(2\text{-Naphthone}\&\beta\text{-carotene})}} \quad \text{S2}$$

Thus, final ϕ_T values are obtained from equation S3

$$\phi_T = \phi_{T(2\text{-naphthone})} [\beta\text{-carotene}] \frac{P_{ET(2\text{-naphthone})}}{P_{ET}} \quad \text{S3}$$